Bidirectional Transport of IgE by CD23 in the Inner Ear of Patients with Meniere's Disease

Na Zhang,*,†,1 Yafeng Lyu,*,†,1 Jia Guo,*,† Jiahui Liu,*,† Yongdong Song,*,† Zhaomin Fan,*,† Xiaofei Li,*,† Na Li,*,†,‡,2 Daogong Zhang,*,†,2 and Haibo Wang*,†,2

Meniere's disease (MD) is a disorder of the inner ear characterized by episodes of spontaneous vertigo, fluctuating hearing loss, and tinnitus. Recent studies have demonstrated that IgE may play a role in the pathogenesis of MD. Patients with MD (n = 103), acoustic neuroma (n = 5), and healthy subjects (n = 72) were recruited into the study. Serum from the participants was analyzed for IgE and type 2–related cytokines. IgE and CD23 expression levels in vestibular end organs of patients, C57BL/6 mice, or mouse HEI-OC1 cells were analyzed. Finally, the role of CD23 in IgE transcytosis was assessed using HEI-OC1 cells. Serum IgE was elevated in patients with MD and positively correlated with clinical symptoms. IL-4, IL-5, IL-10, IL-13, and CD23 levels were increased in patients with MD compared with the control group. In the transcytosis assay, mouse IgE was found to be bidirectionally transported across the HEI-OC1 cell monolayer. Additionally, CD23 downregulation using a small interfering RNA approach significantly reduced the efficiency of IgE transcytosis, suggesting that IgE is transported by CD23. Furthermore, exposure to IL-4 increased CD23 expression and enhanced IgE transcytosis in the HEI-OC1 cells and primary vestibular end organs. Our study indicated that IgE may play a role in the pathophysiology of MD. In addition, CD23-mediated IgE transcytosis in the hair cells may play a critical role in initiating inflammation in the inner ear. Thus, reducing the level of IgE may be a potentially effective approach for MD treatment. *The Journal of Immunology*, **2022, 208: 827–838.**

Meniere's disease (MD) is a heterogeneous and complex peripheral vestibular illness that affects 3.5–513 per 100,000 individuals every year worldwide (1). MD is characterized by episodes of vertigo, sensorineural hearing loss involving low to medium frequencies, tinnitus, and aural fullness (2). Endolymphatic hydrops underlies the classic pathological characteristic of the disease. Several factors have been postulated to be involved in the development of MD, including viral infections, allergies, family history, and autoimmunity (3–6). However, most of the studies are limited by a lack of population-based cohorts and a low number of cases and inner ear tissue specimens. Hence, the pathological mechanism and pathways governing MD remain poorly understood.

Robust associations between allergy and MD have been previously demonstrated (4, 7, 8). Local Ab production in the perilymphatic space has been reported, suggesting the existence of local humoral immunity in the inner ear (9). Additionally, histocompatibility Ags have been implicated in MD pathogenesis, indicating a possible role of the immune system in the disease (10). Although the immunological basis for the allergic origin of MD is not well understood, early studies in the field of otolaryngology demonstrate amelioration of vertigo, tinnitus, and hearing loss in response to the desensitization of patients to inhalant allergens and elimination diet containing food allergens (11). Animals actively sensitized with a specific Ag and subsequently exposed to the same develop endolymphatic hydrops in the inner ear (12). A clinical report has described the relationship between endolymphatic hydrops and an allergic response, which can be triggered by a food allergen–IgE Ab reaction (13).

A significant increase in immune cell populations, including mast cells, basophils, neutrophils, eosinophils, and innate lymphoid cells is observed in allergic inflammation. Furthermore, an imbalance between the Th1 and Th2 cell–mediated immune responses with a skewed Th2 cytokine response increased IL-4, IL-5, and IL-13, and allergy-specific IgE expression is also noted (14). In allergic rhinitis and bronchial asthma, IgE is consistently detected in human nasal washings and bronchoalveolar lavage fluid at markedly increased levels (15, 16). It has been reported that patients with MD exhibit elevated levels of circulating immune complexes (17, 18). IgE is critically involved in the pathophysiology of MD, as evidenced by

*Department of Otolaryngology–Head and Neck Surgery, Shandong Provincial ENT Hospital, Cheeloo College of Medicine, Shandong University, Jinan, Shandong, China; †Shandong Institute of Otorhinolaryngology, Jinan, Shandong, China; and ‡Jinan Central Hospital Affiliated to Shandong University, Jinan, Shandong, China

[1]N.Z. and Y.L. contributed equally to this work.

[2]N.L., D.Z., and H.W. are cosenior authors.

ORCIDs: 0000-0003-3955-3465 (N.Z.); 0000-0002-0620-574X (Y.L.); 0000-0003-0151-2094 (J.L.).

Received for publication July 29, 2021. Accepted for publication November 30, 2021.

This work was supported by the Taishan Scholars Program of Shandong Province (ts20130913) and the Natural Science Foundation of Shandong Province (ZR2020MH17).

H.W. and D.Z. designed the study. N.Z. and N.L. performed experiments. Y.S. and N.L. performed statistical analysis. J.L., X.L., J.G., and Z.F. recruited patients and obtained informed consent from all individuals. N.Z. and Y.L. drafted the manuscript. All authors revised and approved the final version of the manuscript.

Address correspondence and reprint requests to Dr. Haibo Wang, Dr. Daogong Zhang, or Dr. Na Li, Shandong Provincial ENT Hospital, Cheeloo College of Medicine, Shandong University, Huaiyin District, Jinan, Shandong 250022, China (H.W. and D.Z) or Jinan Central Hospital Affiliated to Shandong University, Lixia District, Jinan, Shandong 250013, China (N.L.). E-mail addresses: whboto11@163.com (H.W.), zhangdaogong1978@163.com (D.Z.), or linda831223@163.com (N.L.)

The online version of this article contains supplemental material.

Abbreviations used in this article: AN, acoustic neuroma; ES, endolymphatic sac; HEI-OC1, House Ear Institute–organ of Corti 1; IEM, immunoelectron microscopy; MD, Meniere's disease; qRT-PCR, quantitative real-time PCR; siRNA, small interfering RNA; TEM, transmission electron microscopy; VEO, vestibular end organ.

the effectiveness of anti-IgE therapy in patients with MD (19). Omalizumab is a recombinant humanized mAb that is specific for IgE, and treatment with omalizumab completely resolves debilitating vertigo and nausea without any associated side effects (20).

IgE recognizes allergens via its Fab regions, whereas the effector functions of IgE are regulated via the interactions of the Fc region with the receptors (21). CD23 (also called FcεRII), a 45-kDa type II integral membrane glycoprotein belonging to the C-type lectin-like superfamily, is a low-affinity receptor for IgE (21). The membrane-bound CD23 forms a trimer, allowing CD23 to bind to IgE with high affinity (22). The interaction of CD23 with IgE is involved in regulating several allergic processes (23). For example, CD23 expressed on epithelial cells can amplify the IgE response by transporting IgE across the epithelium via transcytosis, where it can bind and activate FcεRI expressed on mast cells, macrophages, and dendritic cells, thereby promoting allergic inflammation. Furthermore, CD23 can induce the secretion of IL-4 and/or IL-13, thereby contributing to local IgE production (24).

However, until the present, studies have not been conducted to determine the involvement of IgE in MD and the localization of CD23 in the inner ear. In this study, the extent and characteristics of the IgE deposits were studied in the serum and vestibular end organs (VEOs) of patients with MD. Our findings indicate that IgE deposition in VEOs may have a role in the pathophysiology of MD, and the expression of CD23 in hair cells may be crucial for the initiation of inner ear inflammation.

Materials and Methods

Patient population

A total of 103 patients with MD, aged between 27 and 77 y (average age, 52.60 ± 12.68 y), at Shandong Provincial ENT Hospital from January 2017 to December 2019 were enrolled in this study. All of the enrolled patients had been diagnosed with definite MD according to the 2015 diagnostic criteria of the Bárány Society (25). The control group consisted of healthy volunteers (n = 72) and patients with acoustic neuroma (AN; n = 5); all individuals were aged 25–85 y (average age, 53.04 ± 13.93 y), with no history of sudden vertigo, and they lived in the same region and possessed socioeconomic indicators similar to the patient group. The subjects with a history of thermal burns, cancer, a recent bout of influenza, or fever were excluded from the study. The sex distribution and mean age of the patients and controls were not significantly different ($p > 0.05$ for the χ^2 test and t test, Supplemental Table I). Informed consent was obtained from all participants. The study was performed according to the principles of the Declaration of Helsinki revised in 2013 for investigation with humans and the guidelines of the Shandong Provincial ENT Hospital, Cheeloo College of Medicine, Shandong University Ethics Committee (Institutional Review Board ID XYK-20180603).

Tissue sampling and peripheral blood isolation

Patients with MD (n = 6) underwent labyrinthectomy, and the control subjects (n = 5) with AN underwent tumor removal via the translabyrinthine approach. The ampulla, semicircular canal, endolymphatic sac (ES), and maculae were sampled during surgery. Peripheral blood was sampled from all participants in each group and stored in tubes containing EDTA. The serum was immediately separated and stored at −80°C for serum analysis.

Mice

Male C57BL/6 mice were purchased from the Animal Care Committee of Shandong University, Jinan, China. The mice were housed in a temperature-controlled (20–22°C) room, a 12-h light/12-h dark cycle, and had ad libitum access to food and drinking water. Experiments were performed on 6- to 8-wk-old mice and postnatal day 3 mice. All animal experiments were performed according to the protocols approved by the Animal Care Committee of Shandong University (Shandong, China) and were in accordance with the *Guide for the Care and Use of Laboratory Animals for Research Purposes*.

Cell culture and organotypic culture

HEI-OC1 (House Ear Institute–organ of Corti 1) cells, which were derived from murine organ of Corti, were cultured in high-glucose DMEM (Life Technologies, Grand Island, NE) supplemented with 10% FBS (Life Technologies, Grand Island, NE) at 33°C in an atmosphere containing 10% CO_2. The C57BL/6 mice were decapitated at postnatal day 3, their cochlear capsules were removed from the temporal bones to expose the vestibule, and the VEO explants were cultured for 24 h in DMEM/F12 (Life Technologies, Grand Island, NE) supplemented with 10% FBS (Life Technologies, Grand Island, NE) and ampicillin (50 mg/ml, A5354; Sigma-Aldrich, St. Louis, MO), with or without IL-4 (10 ng/ml, ab9729; Abcam, Cambridge, MA) at 37°C in a 5% CO_2 atmosphere.

Extraction of mRNA and quantitative real-time PCR

Total RNA was extracted using an RNA extraction kit (RNeasy Mini QIAcube kit, QIAGEN, Hilden, Germany) from PBMCs, HEI-OC1 cells, and tissues samples. Relative expression of target genes was measured by quantitative real-time PCR (qRT-PCR) that was performed using an Eppendorf AG 22331 PCR machine (Eppendorf, Hamburg, Germany), as reported earlier (26). Briefly, qRT-PCR was performed using SYBR Green Premix Ex Taq (RR42LR, Takara Biotechnology, Shiga, Japan), and *GAPDH* was used as the housekeeping gene. Fold-change differences in mRNA expression were determined using the comparative cycle threshold method (26). The primers for house mice and humans used in this experiment are listed in Table I.

Protein extraction and Western blotting

The total proteins from HEI-OC1 cells and mice cochlear samples were extracted by treating the samples with cold RIPA lysis buffer (Beyotime Institute of Biotechnology, Shanghai, China) supplemented with a protease inhibitor mixture (Sigma-Aldrich, St. Louis, MO) for 30 min at 4°C. The samples were then centrifuged at 12,000 × g for 20 min at 4°C. Protein concentrations were determined using a bicinchoninic acid protein assay kit (Shenergy Biocolor Bioscience & Technology, Shanghai, China). In total, 40 μg of each protein sample was denatured at 99°C for 10 min and resolved in 10% SDS-PAGE gels. The proteins were then transferred to polyvinylidene difluoride membranes (Immobilon-P, IPVH00010; Millipore, Darmstadt, Germany). The membranes were blocked in 5% skim milk for 60 min and then probed with the primary Abs, that is, anti-CD23 Ab (1:1000, ab75487; Abcam, Cambridge, MA) and anti-GAPDH Ab (1:8000, ab8245; Abcam, Cambridge, MA), resuspended in 3% BSA at 4°C overnight. The membranes were incubated with HRP-conjugated goat anti-mouse or goat anti-rabbit IgG Abs (1:2000, ZSGB-BIO, Beijing, China) at room temperature for 60 min. The protein signals were detected using an ECL kit (Millipore, Billerica, MA) and analyzed using ImageJ v1.41 (National Institutes of Health). The blocking, incubation, and washing steps were performed using TBS containing 0.05% Tween 20.

Frozen sections

The inner ear specimens were obtained from patients with MD and AN and were fixed with 4% paraformaldehyde overnight at 4°C. The samples were dehydrated by successive treatment with 15, 20, and 30% sucrose in PBS, and embedded in OCT compound (Tissue-Tek, Sakura Finetek, Torrance, CA). The specimens were sectioned (thickness, 5 μm) with a cryostat (Leica CM 1850, Leica, Nussloch, Germany), and the sections were stored at −80°C.

Immunofluorescence staining

The HEI-OC1 cells were cultured on coverslips to 70–80% confluence or in Transwell inserts to allow polarization and then fixed in 4% paraformaldehyde for 20 min at 4°C. The fixed tissue samples and cells were permeabilized for 30 min with 0.5% Triton X-100 in PBS and blocked with 10% donkey serum for 60 min at room temperature. The samples were incubated with the following primary Abs overnight at 4°C: anti-CD23 (1:200, ab75487; Abcam, Cambridge, MA), anti–myosin VIIa Ab (1:1000, 25-6790; Proteus BioSciences, Ramona, CA), anti–ZO-1 Ab (9664s, Cell Signaling Technology, Boston, MA), anti-Tuj1 Ab (1:1000, MO15013; Neuromics, Edina, MN), anti-human IgE (1:200, sc-52335; Santa Cruz Biotechnology, Santa Cruz, CA), and anti–alpha 1 sodium potassium ATPase (1:400, ab7671; Abcam, Cambridge, MA). Finally, the samples were incubated with the associated fluorescently tagged secondary Abs (1:1000, Invitrogen, Carlsbad, CA) along with DAPI (1:1000, D9542; Sigma-Aldrich, St. Louis, MO) for 60 min in the dark at room temperature. The samples were observed under a laser scanning confocal microscope (Leica SP8, Leica, Wetzlar, Germany). No primary group and IgG group were set up to exclude autofluorescence and nonspecific binding in the utricle of patients with MD and AN (Supplemental Fig. 1A).

Immunohistochemistry analysis

To examine the deposition of IgE, the OCT-embedded VEOs and ES were assessed using a diaminobenzidine detection kit (streptavidin-biotin) kit (SP-9000-D, ZSGB-BIO, Beijing, China). Endogenous peroxidase activity was blocked by incubation for 30 min in 0.3% H_2O_2. Nonspecific binding was blocked by a 20-min incubation with 10% normal goat serum. The sections were stained with rabbit anti-human IgE (1:200, sc-52335; Santa Cruz Biotechnology, Santa Cruz, CA) overnight at 4°C. Next, the sections were incubated with biotinylated anti-rabbit IgG (5 g/ml) for 30 min, followed by an incubation with diaminobenzidine complex for 1 min. The sections were counterstained with hematoxylin, dehydrated, and omitted with neutral balsam (G8590, Solarbio, Beijing, China). Images were obtained using a Leica microscope. No primary group and IgG group were set up to exclude autofluorescence and nonspecific binding in the utricle of patients with MD and AN (Supplemental Fig. 1B).

Transmission electron microscopy and immunoelectron microscopy

Fresh utricles (<1 mm^3 in volume) obtained from patients with MD and AN were fixed with 3% glutaraldehyde fixative solution or fixative for immunoelectron microscopy (IEM). For transmission electron microscopy (TEM), the samples were fixed in 1% osmic acid (OsO_4), dehydrated, soaked, and embedded in Epon 812; ultrathin radial sections were stained with lead citrate and uranyl acetate and observed using a transmission electron microscope (JEOL-1200EX, JEOL, Tokyo, Japan). For IEM, the samples were dehydrated using a graded series of ethanol solutions and embedded in resin. The ultrathin radial sections were fished out onto 150 mesh nickel grids with formvar film, blocked in 1% BSA, and incubated with anti-IgE Ab (1:200, sc-52335; Santa Cruz Biotechnology, Santa Cruz, CA) overnight at 4°C. After incubation with the secondary Ab, the nickel grids were stained in 2% uranium acetate saturated alcohol solution and observed under a transmission electron microscope (JEOL-1200EX, JEOL, Tokyo, Japan). Black golden particles, 10 nm in size, were treated as positive signals.

IgE and cytokine measurement

Venous blood (5 ml) from all of the patients and controls was drawn into procoagulation tubes (Improve Medical, Guangdong, China). The blood samples were collected when the patients with MD were not experiencing an acute episode. The samples were centrifuged at 2000 × *g* for 20 min to separate the serum. The serum levels of IL-4, IL-5, and IL-13 were quantified with commercial ELISA kits (Abcam, Cambridge, MA), following the manufacturer's instructions. Electrochemiluminescence was employed to measure IgE in serum and culture supernatants. An ELISA kit (ab157718, Abcam, Cambridge, MA) was used to measure IgE in the homogenized VEOs of mice.

Transfection of HEI-OC1 cells with small interfering RNA

A mouse-specific CD23 siRNA was used (GenePharma, Shanghai, China) to knock down the expression of CD23 in HEI-OC1 cells. The small interfering RNA (siRNA) sequences included the following: siRNA–negative control, sense, 5′-UUCUCCGAACGUGUCACGUTT-3′, antisense, 5′-ACGUGACACGUUCGGAGAATT-3′; siRNA–Fcer2a-751, sense, 5′-CCAACAGAAGUGCUACUAUTT-3′, antisense, 5′-AUAGUAGCACUUCUGUUGGTT-3′. The cells were seeded in six-well plates to obtain 70% cell confluence after 6 h. Lipofectamine 3000 (10 μl; Invitrogen, Carlsbad, CA) and the siRNA duplexes (500 nmol/L) were added to an appropriate volume of Opti-MEM (Life Technologies, Grand Island, NY) to make a working solution (2 ml), following the manufacturers' protocols. The siRNA efficiency was measured by Western blotting. The cells were further treated with or without IL-4 (ab9729, Abcam, Cambridge, MA). The treated cells were collected for Western blotting, immunofluorescence staining, a cell viability assay, and a transcytosis assay.

Transcytosis assay

IgE transport across monolayer cultured epithelial cells was measured using HEI-OC1 cells grown on Transwell filters (0.4-μm pore size; Thermo Fisher Scientific, Cleveland, OH). Cells (1×10^5 cells/ml) were seeded onto the filter and were incubated in serum-free DMEM at 33°C until transepithelial/endothelial electrical resistance reached 450 Ω/cm^2. For IgE transcytosis, mouse IgE was added to either the apical (5 μg in 200 μl) or basal chamber (10 μg in 500 μl) of the Transwells. After incubation for 30, 60, and 90 min at 33°C or at 4°C, media from the opposite compartments were collected. The concentration of IgE in the media was detected with ELISA as described above.

Cell viability measurement

Cells were seeded at a density of 3000 cells/well in a 96-well plate and allowed to attach overnight for 24 h. The cells were treated with IL-4 (10, 15, 20, 50, 100 ng/ml) for 12, 24, 48, and 72 h, and later transfected with CD23-siRNA or negative control duplexes. After 24 h, the cells were cotreated with IgE (5 μg in 200 ml and 10 μg in 500 ml; as described in *Transfection of HEI-OC1 cells with small interfering RNA*). Cell Counting Kit-8 reagent (10 μl, 96992; Sigma-Aldrich, St. Louis, MO) was added in each well and reacted for 2 h. Absorbance at 450 nm was detected using an ELISA reader (Multiskan MK3, Thermo Fisher Scientific, Cleveland, OH) for cell viability, and the relative cell viability of the negative control group was considered as 100%.

Quantification and image analysis

All quantification in the study was performed in a blinded fashion. Images of the sections were consistently acquired from the same anatomical regions. Three fields that covered a similar area were obtained for the posterior ampulla, upper ampulla, horizontal ampulla, semicircular canal, ES, saccule, and utricle. Images were analyzed using ImageJ v1.41. The eight-bit blue channel image was corrected for background illumination using the eight-bit blue channel of a bright-field image, and a correction method adopted from Landini (2006–2010) was applied to produce an evenly illuminated image (27). A threshold was then applied to the image to measure the total expression identified through specific immunostaining. The same threshold was maintained for all images (MD and AN cases) of sections stained together in the same batch. The percentage of the area examined was used to indicate the IgE load and CD23 expression.

Statistical analysis

The data were statistically analyzed using the SPSS 21.0 statistics software (SPSS, Chicago, IL). Data are presented as mean ± SD for quantitative variables, whereas categorical variables have been shown as numbers and percentages. The variables were compared using non-parametric tests, a Student unpaired *t* test, one-way ANOVA, or a χ^2 test. The correlation analysis between IgE, IL-4, and MD-related variables was analyzed using Spearman's correlation coefficient (*r*). As a threshold, $p < 0.05$ was considered significant.

Results

IgE, IL-4, IL-5, IL-10, and IL-13 are upregulated in patients with MD

Serum samples were collected from patients with MD ($n = 103$) and analyzed for IgE, IL-4, IL-5, IL-10, and IL-13 expression by electrochemiluminescence or ELISA (Table I). The expression profiles of these cytokines were compared with those in healthy individuals ($n = 72$). For the control subjects, serum IgE levels ranged between 0.10 and 126.10 IU/ml, with a mean level of 37.12 IU/ml (SD = 32.64). The IgE levels of the MD group ranged between 0.51 and 892.00 IU/ml, with a mean of 108.56 IU/ml (SD = 175.66). The serum IgE level in patients with MD was significantly different from that in the control group (Fig. 1A). Furthermore, a positive relationship was noted between the level of IgE and grading of endolymphatic hydrops, hearing stage, and functional level (Table II). The levels of serum IL-4, IL-5, IL-10, and IL-13 along with the associated mRNA levels were increased in the MD group relative to those in the control group ($p < 0.05$; Fig. 1B–E), consistent with the qRT-PCR results (Fig. 1F).

Clinical features of patients with MD

Although the average serum IgE level in patients with MD was significantly higher than that in the control group (Fig. 1A), the serum IgE level in most patients with MD was within the normal range. To better illustrate the correlation between IgE and the clinical symptoms of MD, we divided patients with MD into two groups according to the cutoff IgE level (mean ± 2 SD of control group) (Fig. 2A). A total of 75 patients had low basal levels of IgE, and 28 out of 103 patients (27.2%) exhibited high basal levels of IgE (greater than mean + 2 SD = 102.40 IU/ml). However, 4 out of 72 (5.5%) control

Table I. Primer sequences for qRT-PCR

Gene	Forward Primers	Reverse Primers
H-IL-4	5′-CTTTGCTGCCTCCAAGAACAC-3′	5′-GCGAGTGTCCTTCTCATGGT-3′
H-IL-5	5′-CTCTTGGAGCTGCCTACGTG-3′	5′-TTTCCACAGTACCCCCTTGC-3′
H-IL-10	5′-TCAAGGCGCATGTGAACTCC-3′	5′-GATGTCAAACTCACTCATGGCT-3′
H-IL-13	5′-CATCCGCTCCTCAATCCTCT-3′	5′-GCCTTCTGGTTCTGGGTGA-3′
H-CD23	5′-AGGAATTGAACGAGAGGAACGAAGC-3′	5′-GACACCTGCAACTCCATCCTTAGC-3′
H-GAPDH	5′-GAGTCAACGGATTTGGTCGT-3′	5′-TTGATTTTGGAGGGATCTCG-3′
m-CD23	5′-AGAAAGCGTTGCTGCTGTG-3′	5′-GCCAATCCAGGAATCCTTC-3′
m-GAPDH	5′-GTATGACTCCACTCACGG-3′	5′-GGTCTGGCTCCTGGAAGA-3′

H, human; m, house mouse.

individuals exhibited high basal values of IgE. The demographic characteristics of the MD group were compared to evaluate the possible differences according to IgE levels. The correlation between the clinical features of all 103 MD patients with low and high basal levels of IgE was investigated (Table III). No significant differences were noted with respect to distribution in terms of sex, age, and other clinical features for the two groups ($p > 0.05$). However, patients with a high basal level of IgE exhibited a higher frequency of allergy ($p = 0.003$) and severe endolymphatic hydrops ($p = 0.042$) than did those with a low basal level of IgE. The clinical characteristics of patients with high basal levels of IgE are shown in Table IV. In this group, 26 out of the 28 patients were diagnosed with unilateral MD. Furthermore, 17 out of the 28 patients were found to exhibit classic sporadic unilateral MD without migraines and other comorbid autoimmune conditions. Eight of these patients (28.6%) reported a history of allergy. More importantly, the serum expression of IL-4 at the protein and mRNA levels was upregulated in MD patients with a high basal level of IgE compared with that in MD patients with a low basal level of IgE (Fig. 2B, 2F). However, no significant differences were noted in the level of IL-5, IL-10, and IL-13 between the two groups ($p > 0.05$, Fig. 2C–F).

The results of correlation analysis between serum levels of IgE, IL-4, and clinical features of MD patients with varying severity are presented in Table II and Supplemental Table II. In the MD group, we observed a slightly positive correlation between serum IgE and IL-4 levels ($r = 0.26$, $p < 0.05$), ABR threshold ($r = 0.35$, $p < 0.05$), endolymphatic hydrops ($r = 0.35$, $p < 0.05$), and function level ($r = 0.21$, $p < 0.05$) (Table II). However, no correlation was observed between serum IL-4 level and MD-related variables (Supplemental Table II).

IgE deposition in vestibular apparatus of patients with MD

Previous studies have shown that IgE is frequently detected in the mucosal secretions of the airway tract and is upregulated in patients with asthma (16, 28). Hence, we wanted to determine whether IgE depositions were present in the inner ear. Patients with MD with a high basal level of IgE ($n = 3$), those with a low basal level of IgE ($n = 3$), and patients with AN ($n = 5$) were selected for this study. Using immunohistochemical staining, we demonstrated that there was positive IgE staining in the ampulla, macula, semicircular canal, and ES in all patients with MD, thereby indicating that IgE was deposited in the VEOs and ES (Fig. 3A, 3B). Notably, a higher

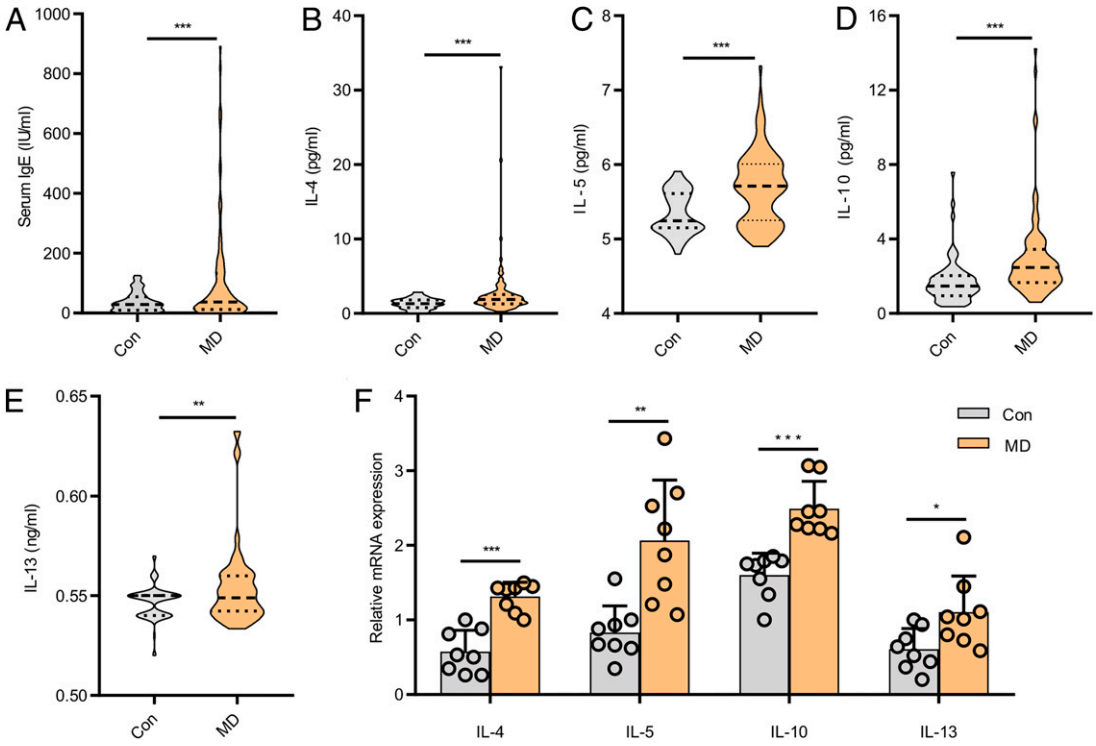

FIGURE 1. IgE and type 2–related cytokines at basal levels in serum. (**A**) Serum levels of IgE in healthy donors ($n = 72$) and patients with MD ($n = 103$) were determined by electrochemiluminescence. (**B–E**) Serum levels of IL-4 (B), IL-5 (C), IL-10 (D), and IL-13 (E) in healthy donors ($n = 72$) and patients with MD ($n = 103$) were determined by ELISA. (**F**) The mRNA levels of IL-4, IL-5, IL-10, and IL-13 in the PBMCs of healthy donors ($n = 8$) and patients with MD ($n = 8$) were determined by qRT-PCR. *$p < 0.05$, **$p < 0.01$, ***$p < 0.001$.

Table II. Correlation between IgE and various factors in patients with Meniere's disease

Variables	*p*	*r*
Age	0.074	0.177
Sex	0.299	−0.103
Side	0.750	0.032
Age of onset	0.150	0.143
Duration	0.122	0.153
Relationship with posture	0.464	0.073
Ophthalmologic symptoms	0.373	0.089
Balance dysfunction	0.182	−0.133
Family history	0.590	0.054
Migraine	0.329	−0.097
Allergy	0.034*	0.209
Autoimmune disease	0.835	0.021
Hypertension	0.157	0.141
Coronary heart disease	0.412	−0.082
Hyperlipidemia	0.720	−0.036
Diabetes	0.280	0.108
Smoking	0.605	−0.052
IL-4	0.007*	0.260
Grading of endolymphatic hydrops	0.000*	0.353
Hearing stage	0.000*	0.350
Functional level	0.034*	0.209

Grading of endolymphatic hydrops using magnetic resonance imaging according to the four-stage grading system. Hearing stage and functional level were measured according to the American Academy Otolaryngology 1995 guidelines. The correlation analysis between IgE and various factors was done using Spearman's correlation coefficient (*r*).

*$p < 0.05$.

deposition of IgE was found in the ampulla and macula of patients with MD than in those with AN (Fig. 3A, 3B). Consistent with the images obtained from immunohistochemical and immunofluorescence staining (Fig. 3C), TEM also confirmed dense deposits in the utricle of patients with MD (Fig. 3D). To define the composition of the dense deposits in patients with MD, we tried to detect an IgE Ag by IEM. Our results showed positive staining near the blood vessels, which further confirmed the results of TEM (Fig. 3E). Taken together, these results demonstrated that IgE deposition increased in the VEOs of patients with MD.

Human VEOs and HEI-OC1 cells express CD23

CD23 is expressed intracellularly and/or at the cell surface in lymphocytes (29), polymorphonuclear leukocytes (30), follicular dendritic cells (31), intestinal epithelial cells (32), and bone marrow stromal cells (33). To assess the expression of CD23, we used the VEOs of patients with MD, HEI-OC1 cells, and cochleae from mice.

The vestibular tissues from patients with MD and AN were stained with a CD23 mAb that recognizes both cell surface and intracellular expression using immunofluorescence. Furthermore, the expression of a marker of hair cells, i.e., myosin7a, was investigated in tissue samples. Colocalization of CD23 with myosin7a in the vestibular tissue indicated the expression of CD23 in hair cells. The specificity and expression pattern of CD23 was, in parallel, observed in the posterior ampulla, upper ampulla, horizontal ampulla, saccule, and utricle (Fig. 4A). The distinct cellular distribution of CD23 in inner ear has not been elucidated in previous studies. CD23 expression was observed in the VEOs of patients with MD in greater frequency and density than in patients with AN (Fig. 4A, 4B). To validate these findings, qRT-PCR was performed, which showed that the relative CD23 mRNA expression in the macula and ampulla of patients with MD was higher than in AN patients (Fig. 4C). In this study, we performed Western blotting to confirm that the cochlear samples and HEI-OC1 cells constitutively expressed CD23

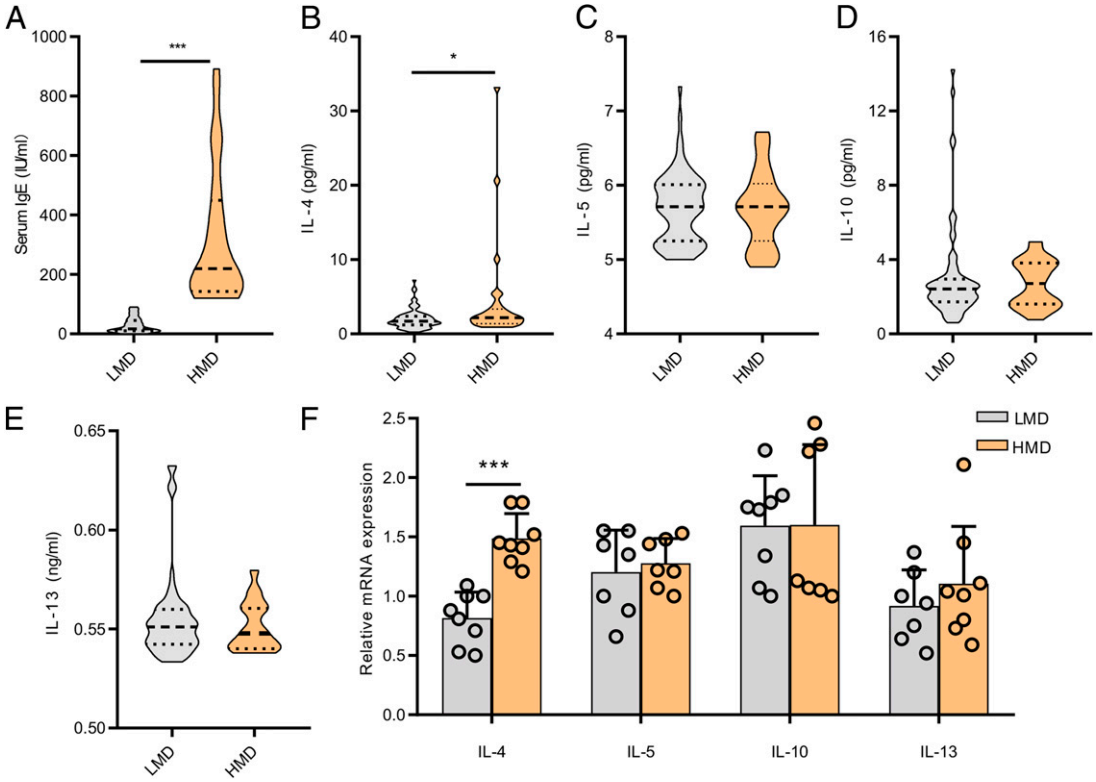

FIGURE 2. IgE and type 2–related cytokines in serum of patients with Meniere's disease. (**A**) Serum levels of IgE in patients with MD ($n = 103$) were determined by electrochemiluminescence. (**B–E**) Serum levels of IL-4 (B), IL-5 (C), IL-10 (D), and IL-13 (E) in patients with LMD ($n = 75$) and HMD ($n = 28$) were determined by ELISA. (**F**) mRNA levels of IL-4, IL-5, IL-10 and IL-13 in the PBMCs of patients with LMD ($n = 8$) and HMD ($n = 8$), as determined by qRT-PCR. *$p < 0.05$, ***$p < 0.001$. HMD, MD with high basal levels of IgE; LMD, MD with low basal levels of IgE; MD, Meniere's disease.

Table III. Clinical features of patients with Meniere's disease with low and high basal levels of IgE

Variables	MD with Low Basal Levels of IgE (n = 75)	MD with High Basal Levels of IgE (n = 28)	p
Age, mean (SD)	52 (11.9)	54 (14.7)	0.433
Sex, n (% women)	44 (58.7)	14 (50.0)	0.430
Side, n (% unilateral)	5 (6.7)	2 (7.1)	0.932
Age of onset (SD)	47.2 (10.8)	46.4 (14.0)	0.787
Duration (h), mean (SD)	3.1 (4.4)	3.1 (2.1)	0.232
Relationship with posture, n (% independence)	4 (5.3)	1 (3.6)	0.711
Ophthalmologic symptoms, n (%)	54 (72.0)	22 (78.6)	0.500
Balance dysfunction, n (%)	63 (84.0)	23 (82.1)	0.821
Basal levels of IgE (SD)	29.0 (26.0)	319.9 (226.0)	0.000*
Family history, n (%)	4 (5.3)	4 (14.3)	0.131
Migraine, n (%)	18 (24.0)	7 (25.0)	0.916
Allergy, n (%)	5 (6.7)	8 (28.6)	0.003
Autoimmune disease, n (%)	5 (6.7)	2 (7.1)	0.932
Hypertension, n (%)	13 (17.3)	9 (32.1)	0.103
Coronary heart disease, n (%)	9 (12.0)	4 (14.3)	0.756
Hyperlipidemia, n (%)	3 (4.0)	2 (7.1)	0.509
Diabetes, n (%)	5 (6.7)	4 (14.3)	0.223
Smoking, n (%)	13 (17.3)	7 (25.0)	0.381
Grading of endolymphatic hydrops, n (%)			
1	5 (6.7)	0 (0.0)	0.042*
2	18 (24.0)	2 (7.1)	0.042*
3	26 (34.7)	9 (32.1)	0.042*
4	26 (34.7)	17 (60.7)	0.042*
Hearing stage, n (%)			
1	14 (18.7)	2 (7.1)	0.055
2	20 (26.7)	2 (7.1)	0.055
3	23 (30.7)	13 (46.4)	0.055
4	17 (22.7)	11 (39.3)	0.055
5	1 (1.3)	0 (0.0)	0.055
Functional level, n (%)			
1	3 (4.0)	0 (0)	0.200
2	14 (18.7)	4 (14.3)	0.200
3	30 (40.0)	11 (39.3)	0.200
4	17 (22.7)	4 (14.3)	0.200
5	9 (12.0)	5 (17.8)	0.200
6	2 (2.7)	4 (14.3)	0.200

Age, age of onset, and basal level of IgE were compared by a Student unpaired t test. Duration was compared by non-parametric tests, and qualitative and categorical variables were compared by a χ^2 test.

*$p < 0.05$.

(45-kDa band; Fig. 4D). In hair cells, CD23 expression was observed on the cell membrane (Fig. 4E). Furthermore, colocalization of CD23 and IgE was observed in patients with MD (Fig. 4F). Thus, we concluded that CD23 was highly expressed in VEOs, indicating that CD23 may play an important role in MD as an IgE receptor in the inner ear epithelial cells.

CD23 transports IgE bidirectionally across the polarized HEI-OC1 cells

The CD23-mediated transepithelial transport mechanism of IgE has been reported in the nasal mucosa in allergic rhinitis, intestinal mucosa during food allergies, and in the respiratory mucosa during allergic asthma (34, 35). Hence, we hypothesized that CD23 may play a pivotal role in the initiation and propagation of IgE deposition in the inner ear. The HEI-OC1 cell line is one of the most commonly used mouse auditory cell lines available for research. HEI-OC1 cells form well-differentiated monolayers with tight junctions and can be used as a model system for transcytosis studies (Fig. 5A). Hence, we used HEI-OC1 cells as a model cell line to examine the transcytosis of IgE. HEI-OC1 cells were grown on Transwell inserts for this purpose. To determine the role of CD23 in transcytosis of IgE, purified mouse IgE was added to either the apical or the basolateral chamber of the Transwell. After IgE addition, the cells were assessed for the appearance of IgE in the opposite chamber using ELISA at 30, 60, or 90 min (Fig. 5B). Interestingly, intact IgE applied to either the apical or the basolateral chamber was transported in the opposite direction across the HEI-OC1 monolayer (Fig. 5C). Transport of IgE was not detected in monolayers incubated at 4°C (Fig. 5C), ruling out the possibility of IgE leakage across HEI-OC1 monolayers.

To determine whether IgE transcytosis was dependent on the expression of CD23 in HEI-OC1 cells, we used the siRNA approach for targeting the CD23 gene in the cells. Using PCR, we confirmed decreased expression of CD23 mRNA in the transfected HEI-OC1 cells (Fig. 5D). A downregulation in CD23 protein expression was also confirmed in the transfected cells (Fig. 5E). The downregulation of CD23 resulted in significant inhibition of transcytosis of IgE in a bidirectional manner ($p < 0.05$; Fig. 5F). Hence, we concluded that IgE that entered through the apical or basolateral transcytotic pathway in HEI-OC1 cells was dependent on CD23 expression.

IL-4 enhances IgE transcytosis

The Th2-type T cells mediate airway allergic inflammation by producing IL-4, IL-5, IL-10, and IL-13. It has been reported that IL-4 can regulate the expression of CD23 in normal B cells (36) and induce IgE production (37); therefore, we investigated the regulation of CD23 in HEI-OC1 cell lines by IL-4. First, the viability of HEI-OC1 cells was greater than 80% at 12, 24, and 36 h after IL-4 (10, 15, 20, 50, 100 ng/ml) stimulation, and it was not different in each group (Fig. 6A). Furthermore, IL-4 did not damage the integrity of the monolayer cell (Supplemental Fig. 1C). The results showed that when HEI-OC1 cells were subjected to IL-4 (10 and 15 ng/ml)

Table IV. Clinical features of patients with Meniere's disease with high basal levels of IgE

Patient	Age (y)	Sex	Side	AO	Duration (h)	RwP	OS	BD	DD	FS	Migraine	Allergy	AD	Hypertension	CHD	Dyslipidemia	Diabetes	Smoking	GEH	HS	FL	IgE (IU/ml)
1	32	M	R	28	3.5	Y	Y	Y	1	N	N	Y	N	N	N	N	N	N	2	3	5	120
2	54	M	L	34	2.5	Y	Y	Y	3	N	Y	Y	N	N	N	N	Y	N	3	3	4	129.8
3	51	F	L	41	0.15	Y	Y	Y	3	N	Y	Y	N	Y	Y	N	N	N	1	4	3	133.3
4	65	M	L	62	3	Y	N	Y	3	N	Y	N	N	Y	N	N	N	Y	3	3	3	134.7
5	34	M	R	40	0.3	Y	Y	Y	3	N	N	N	N	N	N	Y	N	N	2	4	3	134.7
6	61	F	L	60	0.3	Y	Y	Y	3	N	N	N	N	Y	N	N	Y	N	2	3	2	136.7
7	63	M	L	36	2	Y	Y	Y	3	N	N	N	N	N	N	Y	Y	N	3	4	3	136.8
8	34	F	R	31	3	Y	Y	Y	3	N	N	Y	N	N	N	N	N	N	2	4	3	161.1
9	54	F	L	49	3	Y	Y	N	3	N	N	N	N	N	N	N	N	N	3	3	6	169.1
10	27	F	B	15	5	Y	N	N	3	Y	N	N	N	N	N	N	N	N	3	3	4	169.3
11	77	F	L	62	10	Y	Y	Y	3	N	N	Y	N	Y	N	N	N	N	2	3	5	178.2
12	66	F	R	36	3	Y	N	Y	3	N	N	N	Y	N	N	N	N	Y	3	3	3	181
13	75	F	L	38	2.5	Y	Y	Y	3	Y	Y	N	N	Y	N	N	N	Y	3	3	6	185.2
14	56	F	B	54	1.5	Y	Y	Y	3	N	Y	N	N	N	N	N	N	N	1	1	6	213.6
15	46	1	L	46	6.5	Y	N	Y	2	N	N	Y	N	N	N	N	N	N	2	2	3	224.8
16	56	M	L	52	1	Y	Y	Y	1	Y	N	N	N	N	N	N	N	N	3	4	3	245.60
17	72	M	R	68	5	Y	Y	Y	2	N	N	N	N	N	Y	N	N	Y	3	4	5	263.4
18	63	M	L	59	2	Y	Y	Y	3	N	N	N	N	N	N	N	N	Y	3	3	2	303.70
19	51	M	L	49	1	Y	Y	Y	3	N	N	N	N	N	N	N	Y	N	2	4	3	350.1
20	33	F	L	31	2.5	N	Y	N	3	N	N	N	N	N	N	N	N	N	3	3	5	358.80
21	56	M	R	54	5	Y	Y	Y	3	Y	N	N	N	N	N	N	N	N	3	3	2	382.30
22	40	F	L	40	2	Y	N	Y	3	N	N	Y	Y	N	Y	N	N	N	2	2	2	471.5
23	69	F	R	66	3.5	Y	Y	Y	3	N	N	N	N	Y	N	N	N	N	2	1	5	497.4
24	71	F	L	65	5	Y	Y	Y	3	N	N	N	N	Y	N	N	N	N	3	4	4	630.2
25	30	F	R	27	2	Y	Y	N	3	N	Y	N	N	N	N	N	N	N	3	4	4	667.5
26	65	M	L	55	3	Y	Y	Y	2	N	N	Y	N	N	Y	N	N	N	3	4	6	667.8
27	52	M	L	39	4.5	Y	Y	N	3	N	N	N	N	Y	N	N	N	Y	3	4	3	819
28	65	M	L	62	3	Y	N	Y	3	N	Y	N	N	Y	N	N	N	Y	3	3	3	892

AD, autoimmune disease; AO, age of onset; B, bilateral; BD, balance dysfunction; CHD, coronary heart disease; F, female; FL, function level; FS, family history; GEH, grading of endolymphatic hydrops; HS, hearing stage; L, left; M, male; N, no; OS, ophthalmologic symptoms; R, right; RwP, relationship with posture; Y, yes.

stimulation for 12 h, CD23 mRNA expression, as measured by RT-PCR, was significantly upregulated (Fig. 6B). This result was in accordance with the Western blots (Fig. 6C). We further examined whether IL-4 treatment stimulates the transcytosis of IgE across HEI-OC1 cells. To show this effect, the HEI-OC1 monolayers were treated with or without IL-4 (10 ng/ml) before IgE was added. The transcytosis of mouse IgE was significantly enhanced in both apical-to-basolateral and basolateral-to-apical directions upon exposure to IL-4 for 12 h at 33°C in comparison with that of untreated cells (Fig. 6D). We also tested the mRNA expression of type 2 immune response–related cytokines in VEOs and ES by RT-PCR and observed that IL-4 mRNA expression was elevated in both the macula and ampulla of patients with MD compared with those in AN patients (Fig. 6E).

Finally, we cultured primary VEOs from C57BL/6 mice and stimulated them with IL-4 for 24 h. Our results showed that IL-4 treatment induced expression of CD23 mRNA and protein (Fig. 6F, 6G). Moreover, IL-4 treatment increased the level of IgE in the homogenate of VEOs (Fig. 6H). Collectively, these results suggest that IL-4 plays a role in the transcytosis and expression of IgE.

Discussion

MD is a heterogeneous and complex disease that is characterized by the involvement of multiple pathways and cellular components in its pathogenesis (2). There is increasing evidence that IgE autoantibodies are involved in the pathogenesis of MD, as well as other autoimmune inner ear diseases (13, 38). In this study, serum IgE levels were found to be upregulated in patients with MD. Patients with a high basal level of IgE exhibited a high frequency of allergies, indicating that allergies and the elevated levels of serum IgE may be closely related to MD. More importantly, a positive relationship was noted between the level of IgE and grading of endolymphatic hydrops, hearing stage, and functional level, indicating that IgE may play a role in the pathogenesis of MD, and monitoring serum IgE levels may serve as a biomarker of MD diagnosis and therapeutic efficacy.

Th2 cell predominance, along with the overproduction of cytokines such as IL-4, may prevent the development of cellular immunity against microorganisms and drive chronic allergic diseases such as asthma and atopic dermatitis (39). Cytokines IL-4, IL-5, and IL-13 can further promote B cell class switching to increase IgE production (40). Munno et al. (41) described an increase in the levels of TNF-α, IL-4, and IL-5 in patients with migraines. IL-4 expression is also associated with MD (42). In this study, we found that type 2–related cytokines were higher in serum and VEOs of patients with MD, which was consistent with the results of prior studies. Hence, we concluded that MD was strongly associated with the expression of IgE and cytokines. Increased expression of these molecules may also be induced in the inner ear in response to IgE deposition and may be responsible for the high levels of serum IgE.

The ES is considered to be the primary immunological tissue structure of the inner ear (43); however, IgE deposition was detected in the VEOs and not in the ES. Deposition of IgE may induce an inflammatory reaction and culminate in increased vascular permeability and the subsequent development of hydrops. We hypothesize that the VEOs are the sites of immune reaction and repeated inflammatory reactions may result in VEO dysfunction and eventually result in MD development. Interestingly, we noted that IgE was deposited in the VEOs of MD patients with both high serum IgE and low serum IgE levels, suggesting that serum IgE level does not affect the deposition of IgE in the inner ear. Hence, IgE in VEOs may be produced in situ rather than via the translocation of circulating IgE. However, the mechanism of IgE production in the inner ear requires further analysis. Barring the area around the blood vessels, IgE was also deposited in, and below, the hair cells. As IgE and

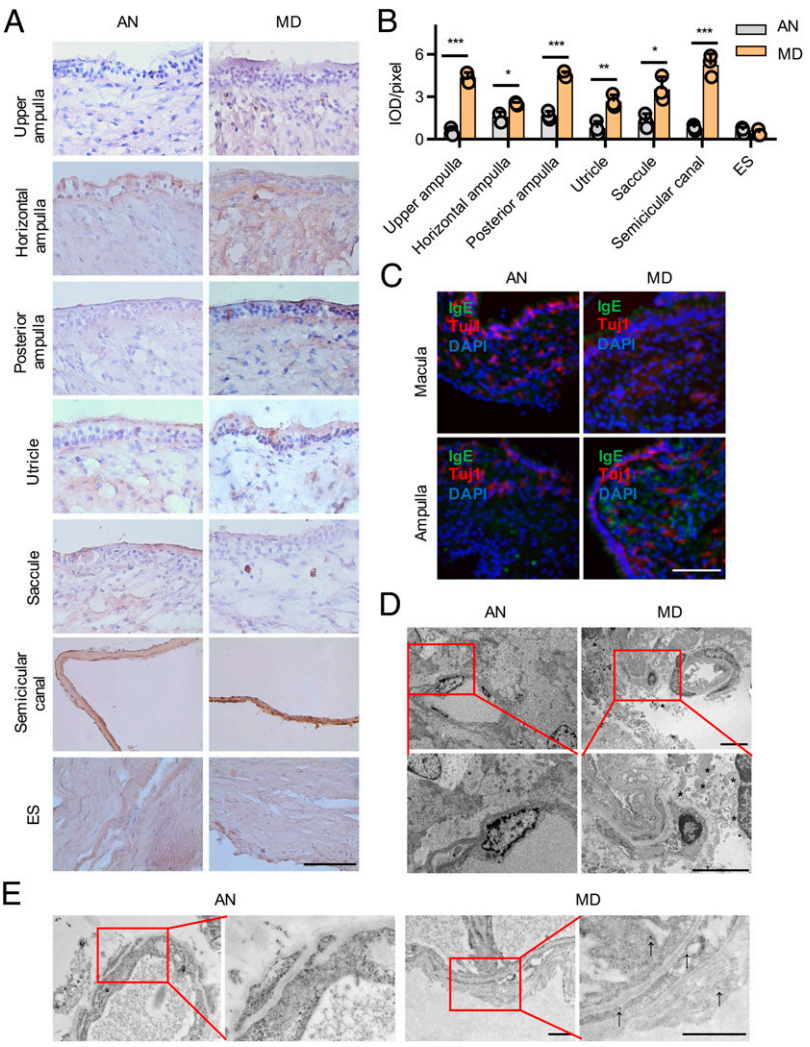

FIGURE 3. Constitutive expression of IgE in human vestibular apparatus. (**A**) The distribution of IgE in the VEOs and ES was determined by immunohistochemistry. A stronger signal of IgE was observed in the VEOs in the patients with MD than in patients with AN. Scale bar, 100 μm. (**B**) Densitometric quantification of the mean ratio of IgE expressed as mean ± SD ($n = 3$). (**C**) The distribution of IgE (in green) in macula and ampulla as determined by immunofluorescence staining. The axons of neurons were stained with Tuj1 (in red), and the nuclei were stained with DAPI (in blue). Scale bar, 100 μm. (**D**) The ultrastructure of saccule was observed by transmission electron microscopy. Immune complex deposition was detected around the vessels in the MD tissue samples. Asterisks mark the immune complex deposition. Scale bars, 2 μm. (**E**) The ultrastructure of utricle was observed by immunoelectron microscopy. Arrows indicate the golden particles. Scale bars, 1 μm. $*p < 0.05$, $**p < 0.01$, $***p < 0.001$. AN, acoustic neurinoma; EC, endothelial cell; ES, endolymphatic sac; HA, horizontal ampulla; MD, Meniere's disease; PA, posterior ampulla; S, saccule; SC, semicircular canal; U, utricle; UA, upper ampulla.

CD23 were colocalized in the hair cells, we predicted that hair cells may be involved in the transport of IgE in the inner ear.

Although CD23 is known to be expressed in several cell types, including lymphocytes, eosinophils, and monocytes (35), its expression and function in the inner ear have remained relatively undefined. Increased expression levels of CD23 in inflammatory bowel disease and cow milk–induced enteropathy have been reported (44). In this study, we have systemically confirmed the constitutive expression of CD23 in human VEOs, mice cochlea, and HEI-OC1 cells. We found that CD23 expression was mainly observed on the hair cell membrane, suggesting that CD23 may function as an intracellular IgE receptor in the inner ear.

The function of CD23 has been extensively studied; for example, CD23-mediated transepithelial transport of IgE is observed in the nasal mucosa of patients with allergic rhinitis, in the intestinal mucosa of patients with food allergies, and in the respiratory mucosa of patients with allergic asthma (32, 34, 45). However, there is a paucity of information describing the link between CD23 expression in the vestibular hair cells and the functional outcome. In vestibular hair cells, CD23 was observed to be localized at both the apical and basolateral membranes, suggesting that IgE may be transported in both directions across the epithelium. As we were unable to obtain sufficient inner ear tissue samples, we used the HEI-OC1 cell line to study CD23 function in the inner ear. Notably, the bidirectional transcytosis of the exogenously applied IgE was observed in the HEI-OC1 cells. Further studies are required to determine the mechanism by which CD23 releases IgE at the cell surface after transcytosis.

Furthermore, we noted increased expression of CD23 in the VEOs of patients with MD. This observation may partially explain the elevated IgE in VEOs of patients with MD. Prior research has demonstrated that individuals with asthma displayed an elevated level of CD23 in monocytes compared with healthy individuals (46, 47). In contrast, Tantisira and colleagues (48) demonstrated that elevated IgE levels observed in asthmatic patients were associated with reduced CD23 expression. We predict that different CD23 variants contribute to these contrasting effects. Interestingly, human CD23 exists in two forms, i.e., CD23a and CD23b (49). CD23b is a splice variant of CD23a that differs from CD23a, as it lacks a tyrosine motif in the N-terminal cytoplasmic region, which is considered important for endocytic signaling (50). These two molecules are functionally different; CD23a facilitates the endocytic uptake of IgE, whereas CD23b splice variants are associated with IgE-mediated phagocytosis (49). Murine CD23 exists in seven forms. This study does not rule out the expression of CD23 variants, and in situ hybridization studies are necessary to conclusively determine whether CD23 isoforms are expressed by specific cell types in vivo.

CD23 is involved in regulating IgE synthesis in B cells (51), development of extrinsic allergy alveolitis in alveolar macrophages, and in the response to stimulation of the airway smooth muscle cells (52). Membrane-bound CD23 is thought to undergo oligomerization, a phenomenon that may affect IgE binding (53). The mechanism and extent of this oligomerization remain to be defined, and this complicates further assessment of protein–protein interactions. CD23 also exhibits a complicated array of interaction partners that

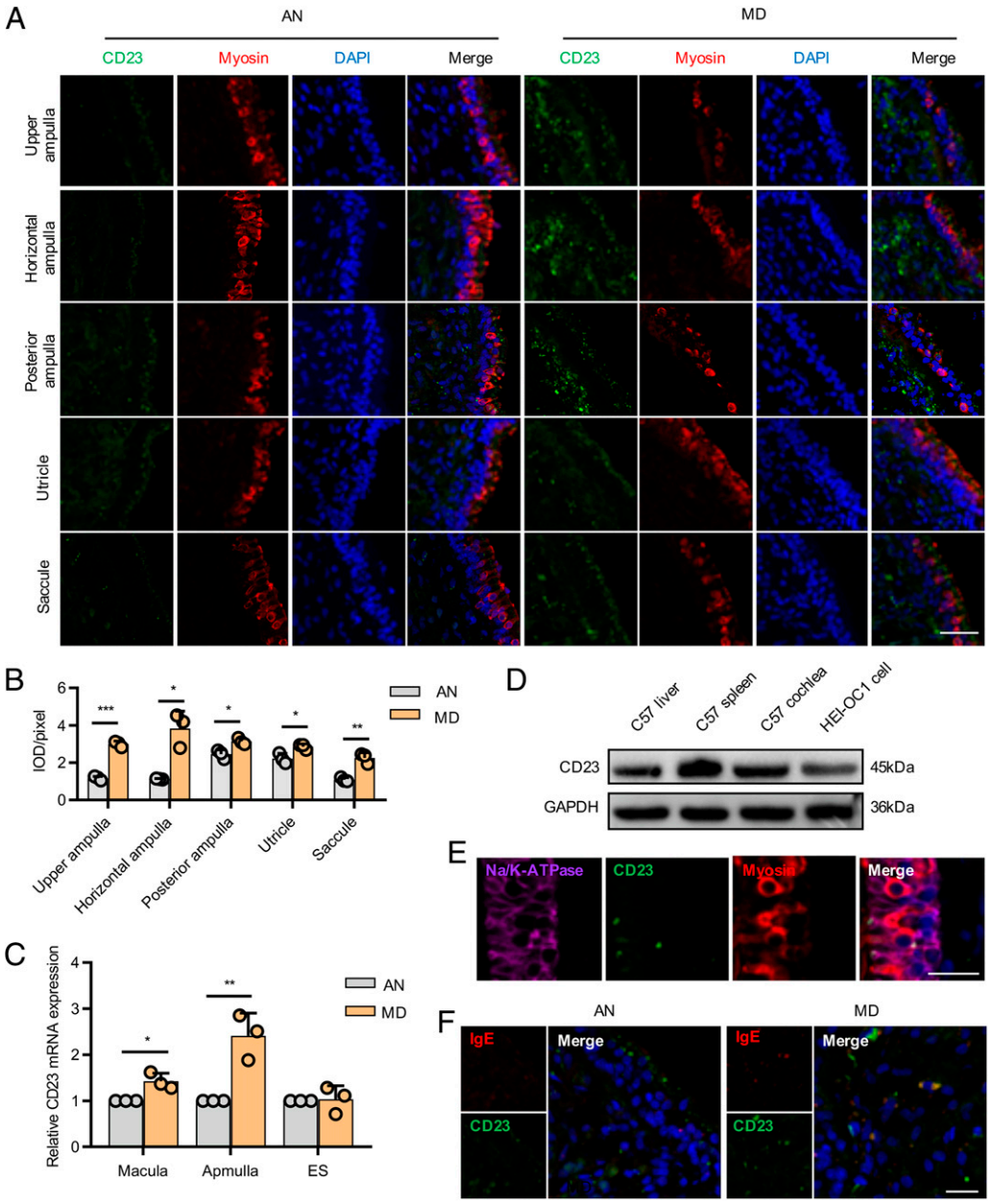

FIGURE 4. Expression of CD23 in the inner ear. (**A**) The distribution of CD23 (in green) in VEOs was determined by immunofluorescence. A stronger signal of IgE was observed in the patients with MD than in patients with AN. The hair cells were stained with myosin (in red), and the nuclei were stained with DAPI (in blue). Scale bar, 50 μm. (**B**) Densitometric quantification of the mean ratio of CD23 expressed as mean ± SD ($n = 3$). (**C**) The mRNA levels of CD23 in the macula, ampulla, and ES in patients with MD ($n = 3$) and AN ($n = 3$) were determined by qRT-PCR. (**D**) Western blotting analysis of CD23 expression in the mice samples and HEI-OC1 cells. GAPDH was used as a loading control. (**E**) The distribution of CD23 (in green) in utricles of patients with MD was determined by immunofluorescence. The hair cells were stained with myosin (in red), the cell membrane was stained with Na/K-ATPase (in purple), and the nuclei were stained with DAPI (in blue). Scale bar, 20 μm. (**F**) The colocalization of CD23 and IgE was observed by immunofluorescence in the VEOs of patients with MD. Scale bar, 50 μm. $^{*}p < 0.05$, $^{**}p < 0.01$, $^{***}p < 0.001$. AN, acoustic neurinoma; HA, horizontal ampulla; MD, Meniere's disease; PA, posterior ampulla; S, saccule; U, utricle; UA, upper ampulla.

could affect membrane distribution or stabilization (23). Hence, based on the results of this study and prior reports, we predict that CD23 may play a significant role in inner ear inflammation. Further studies are required to elucidate the functional consequences of the mechanism identified in this study.

More importantly, we found that IL-4 upregulates CD23 expression in HEI-OC1 cells and VEOs. The increased expression of induced CD23 was potentially due to activation of the IL-4 enhancer element on the CD23 gene (54). Upregulation of CD23 expression is one of the hallmarks of IL-4–induced immune responses and is believed to have important roles in the pathogenesis of asthma (45). Notably, we observed that the IL-4 level was positively correlated with the serum IgE level. Furthermore, IL-4–mediated upregulation of CD23 expression also enhanced the transcytosis of IgE across the HEI-OC1 monolayer. Conversely, CD23 deficiency significantly decreased IgE transport. These results show that the transepithelial transport of IgE is mediated by the CD23 expressed in HEI-OC1 cells. Although we did not obtain hair cell culture samples from patients with MD, IgE presence in human VEOs of patients with MD has been documented. It is very likely that expression of CD23 might enhance

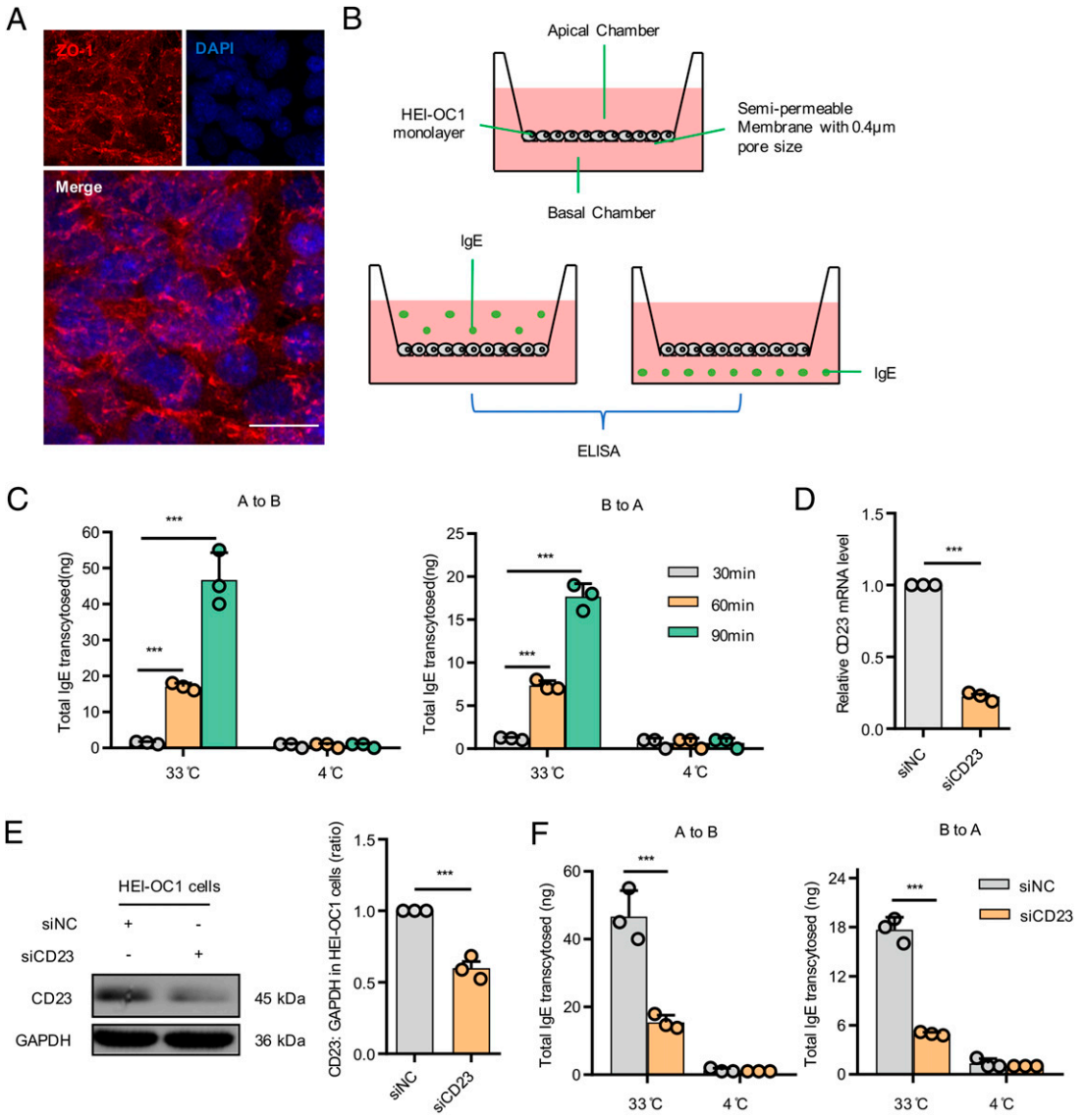

FIGURE 5. Transcytosis of IgE by CD23 in HEI-OC1 cells. (**A**) Immunofluorescence for assessing ZO-1 expression. The HEI-OC1 cells were grown on a Transwell insert and incubated with ZO-1 Ab (in red) to visualize tight junctions. Nuclei were stained with DAPI. Scale bar, 50 μm. (**B**) Diagram of the Transwell. Transcytosis of IgE in the HEI-OC1 cell monolayer. Cells were grown on the filter supports in Transwells to polarize the cells. IgE was added to the apical (A) or basal (B) wells of the Transwell, and supernatant from the opposite Transwell was collected to measure IgE concentration by ELISA. (**C**) IgE was added to the apical (5 μg in 200 μl) or basal (10 μg in 500 μl) wells of the Transwell, and supernatant from the opposite Transwell was collected to measure IgE concentration by ELISA over a duration of 30, 60, and 90 min at 33 or 4°C. (**D**) CD23 mRNA expression in HEI-OC1 cells treated with or without CD23 siRNA. (**E**) Western blotting to analyze CD23 expression in HEI-OC1 cells treated with or without CD23 siRNA. GAPDH was used as a loading control. (**F**) Supernatants from the opposite Transwells were collected to measure IgE concentration by ELISA in HEI-OC1 cells treated with or without CD23 siRNA at 33 or 4°C. ***$p < 0.001$.

transport function in hair cells in MD. Our results were in agreement with findings of IL-4–enhanced IgE transcytosis in the intestinal epithelial cells (24, 32). Hence, elevated serum IL-4 may be responsible for the augmentation of CD23 expression and IgE deposition in MD.

The capacity of CD23 to facilitate an allergic inflammatory response in the inner ear may have important implications for food allergies as well. Indeed, i.v. infusion of CD23-specific Ab has previously been proposed as a therapeutic strategy in asthma, and CD23 is possibly involved in the signaling leading to proinflammatory responses (45, 55). However, there has been no concrete in vivo evidence supporting the function of CD23 to directly initiate or facilitate allergic inflammation in the inner ear. CD23 expression has been detected in intestinal and airway epithelial cells (24, 34) and, in this study, we demonstrated that CD23 expressed on hair cells acts as a receptor for the binding of IgE in vivo and bidirectional transporter of IgE across hair cells in vitro.

There are several issues that remain unaddressed in the CD23-mediated inner ear allergic inflammatory response. First, IgE that can crosslink CD23 on hair cells may initiate signaling cascades contributing to the induction of proinflammatory cytokines and chemokines. Cytokines, in turn, may cause increased CD23 expression and transcytosis of IgE, resulting in the recruitment of more immune cells into the inner ear, forming a positive feedback loop culminating in inflammation. Second, the role of CD23 in hair cells in the development of allergic inflammation in vivo has remained elusive. A working model can be developed based on the results of this study. Allergen-specific IgE is secreted by plasma cells. CD23 then mediates transcytosis of IgE, which is capable of activating hair cells and immune effector

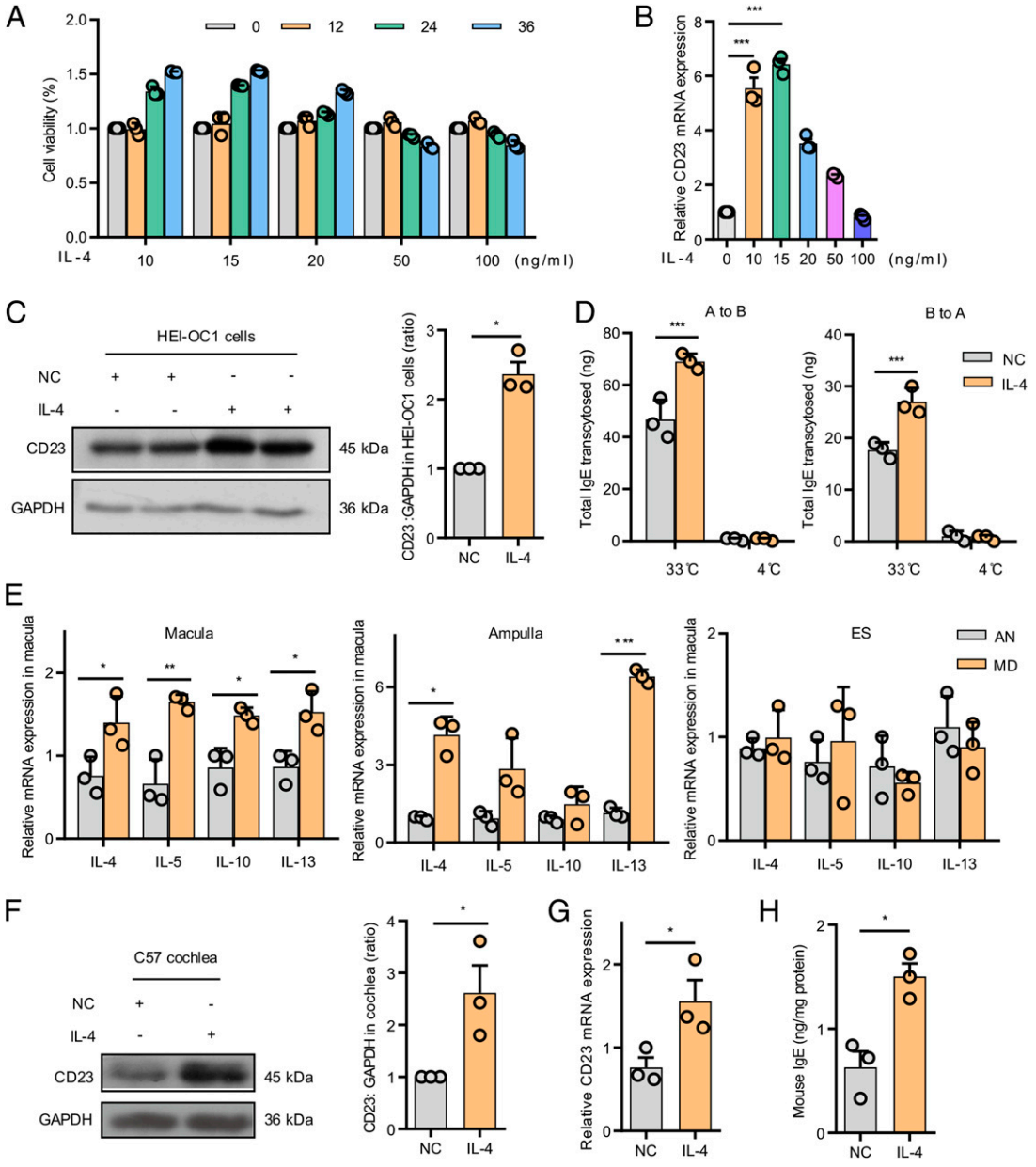

FIGURE 6. IL-4 enhances IgE transcytosis. (**A**) Cell Counting Kit-8 assay conducted for assessing the viability of HEI-OC1 cells exposed to IL-4 (10, 15, 20, 50, or 100 ng/ml) for 12, 24, or 36 h. (**B**) CD23 mRNA expression in the HEI-OC1 cells exposed to IL-4 (10, 15, 20, 50, or 100 ng/ml) for 12 h. (**C**) Western blotting to check for the expression of CD23 in HEI-OC1 cells treated with or without IL-4. GAPDH was used as the loading control. (**D**) Supernatants from the opposite Transwells were collected to measure IgE concentration by ELISA in HEI-OC1 cells treated with or without IL-4 at 33 or 4°C. (**E**) The mRNA levels of IL-4, IL-5, IL-10, and IL-13 in the macula, ampulla, and ES of patients with MD ($n = 3$) and AN ($n = 3$) were determined by qRT-PCR. (**F**) Western blot analysis to analyze CD23 expression in primary VEOs of mice exposed to IL-4 (10 ng/ml) for 24 h; GAPDH was used as the loading control. (**G**) CD23 mRNA expression in primary VEOs of mice exposed to IL-4 (10 ng/ml) for 24 h. (**H**) IgE levels in mouse VEO homogenates were determined by ELISA. *$p < 0.05$, **$p < 0.01$, ***$p < 0.001$.

cells, such as T cells and perivascular resident macrophage-type melanocytes. Moreover, cytokines secreted by activated immune cells may provide feedback to the hair cell epithelium to increase the expression of CD23 and to support the influx of a new wave of inflammatory and adaptive immune cells into the inner ear.

Based on the results of this study, IgE and Th2-relative cytokine IL-4 may be associated with MD. Hence, monitoring their levels may serve as a biomarker of diagnosis, and thereby influence therapeutic efficacy of MD. Due to the significance of IgE in MD, it may have implications in future therapeutic strategies as well. In conclusion, we demonstrated that elevated levels of IgE and proinflammatory cytokines are detected in the peripheral blood and VEOs of patients with MD. Furthermore, CD23 expressed on hair cells functioned as a specific bidirectional IgE transporter, which was regulated by IL-4. Thus, IgE levels may serve as useful biomarkers to assess the progression of MD. This study also suggests that blocking CD23-mediated IgE transport may be a potentially important target for the treatment of MD.

Acknowledgments

The authors thank all patients and healthy controls participating in this study.

Disclosures

The authors have no financial conflicts of interest.

References

1. Alexander, T. H., and J. P. Harris. 2010. Current epidemiology of Meniere's syndrome. *Otolaryngol. Clin. North Am.* 43: 965–970.
2. Sajjadi, H., and M. M. Paparella. 2008. Meniere's disease. *Lancet* 372: 406–414.
3. Requena, T., J. M. Espinosa-Sanchez, S. Cabrera, G. Trinidad, A. Soto-Varela, S. Santos-Perez, R. Teggi, P. Perez, A. Batuecas-Caletrio, J. Fraile, et al. 2014. Familial clustering and genetic heterogeneity in Meniere's disease. *Clin. Genet.* 85: 245–252.
4. Derebery, M. J., and K. I. Berliner. 2010. Allergy and its relation to Meniere's disease. *Otolaryngol. Clin. North Am.* 43: 1047–1058.
5. Gazquez, I., A. Soto-Varela, I. Aran, S. Santos, A. Batuecas, G. Trinidad, H. Perez-Garrigues, C. Gonzalez-Oller, L. Acosta, and J. A. Lopez-Escamez. 2011. High prevalence of systemic autoimmune diseases in patients with Menière's disease. *PLoS One* 6: e26759.
6. Peroutka, S. J. 2004. Migraine: a chronic sympathetic nervous system disorder. *Headache* 44: 53–64.
7. Keles, E., A. Gödekmerdan, T. Kalidağ, I. Kaygusuz, S. Yalçin, H. Cengiz Alpay, and M. Aral. 2004. Meniere's disease and allergy: allergens and cytokines. *J. Laryngol. Otol.* 118: 688–693.
8. Tyrrell, J. S., D. J. Whinney, O. C. Ukoumunne, L. E. Fleming, and N. J. Osborne. 2014. Prevalence, associated factors, and comorbid conditions for Ménière's disease. *Ear Hear.* 35: e162–e169.
9. Harris, J. P. 1984. Immunology of the inner ear: evidence of local antibody production. *Ann. Otol. Rhinol. Laryngol.* 93: 157–162.
10. Arweiler, D. J., K. Jahnke, and H. Grosse-Wilde. 1995. [Meniere disease as an autosome dominant hereditary disease]. *Laryngorhinootologie* 74: 512–515.
11. Powers, W. H. 1973. Allergic factors in Meniere's disease. *Trans. Am. Acad. Ophthalmol. Otolaryngol.* 77: ORL22–ORL29.
12. Egami, N., A. Kakigi, T. Takeda, S. Takeda, R. Nishioka, M. Hyodo, and T. Yamasoba. 2014. Type 1 allergy-induced endolymphatic hydrops and the suppressive effect of H1-receptor antagonist (olopatadine hydrochloride). *Otol. Neurotol.* 35: e104–e109.
13. Li, G., D. You, J. Ma, W. Li, H. Li, and S. Sun. 2018. The role of autoimmunity in the pathogenesis of sudden sensorineural hearing loss. *Neural Plast.* 2018: 7691473.
14. Gould, H. J., and B. J. Sutton. 2008. IgE in allergy and asthma today. *Nat. Rev. Immunol.* 8: 205–217.
15. Crimi, E., A. Scordamaglia, P. Crimi, S. Zupo, and S. Barocci. 1983. Total and specific IgE in serum, bronchial lavage and bronchoalveolar lavage of asthmatic patients. *Allergy* 38: 553–559.
16. Rondón, C., J. J. Romero, S. López, C. Antúnez, E. Martín-Casañez, M. J. Torres, C. Mayorga, R. R-Pena, and M. Blanca. 2007. Local IgE production and positive nasal provocation test in patients with persistent nonallergic rhinitis. *J. Allergy Clin. Immunol.* 119: 899–905.
17. Brookes, G. B. 1986. Circulating immune complexes in Meniere's disease. *Arch. Otolaryngol. Head Neck Surg.* 112: 536–540.
18. Derebery, M. J., V. S. Rao, T. J. Siglock, F. H. Linthicum, and R. A. Nelson. 1991. Menière's disease: an immune complex-mediated illness? *Laryngoscope* 101: 225–229.
19. Siebenhaar, F., W. Kühn, T. Zuberbier, and M. Maurer. 2007. Successful treatment of cutaneous mastocytosis and Ménière disease with anti-IgE therapy. *J. Allergy Clin. Immunol.* 120: 213–215.
20. Babu, K. S., S. H. Arshad, and S. T. Holgate. 2001. Omalizumab, a novel anti-IgE therapy in allergic disorders. *Expert Opin. Biol. Ther.* 1: 1049–1058.
21. Sutton, B. J., and A. M. Davies. 2015. Structure and dynamics of IgE-receptor interactions: FcεRI and CD23/FcεRII. *Immunol. Rev.* 268: 222–235.
22. Dierks, S. E., W. C. Bartlett, R. L. Edmeades, H. J. Gould, M. Rao, and D. H. Conrad. 1993. The oligomeric nature of the murine Fc epsilon RII/CD23. Implications for function. *J. Immunol.* 150: 2372–2382.
23. Acharya, M., G. Borland, A. L. Edkins, L. M. Maclellan, J. Matheson, B. W. Ozanne, and W. Cushley. 2010. CD23/FcεRII: molecular multi-tasking. *Clin. Exp. Immunol.* 162: 12–23.
24. Tu, Y., S. Salim, J. Bourgeois, V. Di Leo, E. J. Irvine, J. K. Marshall, and M. H. Perdue. 2005. CD23-mediated IgE transport across human intestinal epithelium: inhibition by blocking sites of translation or binding. *Gastroenterology* 129: 928–940.
25. Lopez-Escamez, J. A., J. Carey, W. H. Chung, J. A. Goebel, M. Magnusson, M. Mandalà, D. E. Newman-Toker, M. Strupp, M. Suzuki, F. Trabalzini, et al.; Classification Committee of the Barany Society; Japan Society for Equilibrium Research; European Academy of Otology and Neurotology (EAONO); Equilibrium Committee of the American Academy of Otolaryngology-Head and Neck Surgery (AAO-HNS); Korean Balance Society. 2015. Diagnostic criteria for Menière's disease. *J. Vestib. Res.* 25: 1–7.
26. Zhang, N., J. Cai, L. Xu, H. Wang, and W. Liu. 2020. Cisplatin-induced stria vascularis damage is associated with inflammation and fibrosis. *Neural Plast.* 2020: 8851525.
27. Zotova, E., V. Bharambe, M. Cheaveau, W. Morgan, C. Holmes, S. Harris, J. W. Neal, S. Love, J. A. R. Nicoll, and D. Boche. 2013. Inflammatory components in human Alzheimer's disease and after active amyloid-β_{42} immunization. *Brain* 136: 2677–2696.
28. Balzar, S., M. Strand, D. Rhodes, and S. E. Wenzel. 2007. IgE expression pattern in lung: relation to systemic IgE and asthma phenotypes. *J. Allergy Clin. Immunol.* 119: 855–862.
29. Liu, C., K. Richard, M. Wiggins, X. Zhu, D. H. Conrad, and W. Song. 2016. CD23 can negatively regulate B-cell receptor signaling. *Sci. Rep.* 6: 25629.
30. Lantero, S., G. Alessandri, D. Spallarossa, L. Scarso, and G. A. Rossi. 2000. Stimulation of eosinophil IgE low-affinity receptor leads to increased adhesion molecule expression and cell migration. *Eur. Respir. J.* 16: 940–946.
31. Sukumar, S., D. H. Conrad, A. K. Szakal, and J. G. Tew. 2006. Differential T cell-mediated regulation of CD23 (FcεRII) in B cells and follicular dendritic cells. *J. Immunol.* 176: 4811–4817.
32. Li, H., A. Nowak-Wegrzyn, Z. Charlop-Powers, W. Shreffler, M. Chehade, S. Thomas, G. Roda, S. Dahan, K. Sperber, and M. C. Berin. 2006. Transcytosis of IgE-antigen complexes by CD23a in human intestinal epithelial cells and its role in food allergy. *Gastroenterology* 131: 47–58.
33. Fourcade, C., M. Arock, S. Ktorza, F. Ouaaz, H. Merle-Béral, F. Mentz, E. Kilchherr, P. Debré, and M. D. Mossalayi. 1992. Expression of CD23 by human bone marrow stromal cells. *Eur. Cytokine Netw.* 3: 539–543.
34. Palaniyandi, S., E. Tomei, Z. Li, D. H. Conrad, and X. Zhu. 2011. CD23-dependent transcytosis of IgE and immune complex across the polarized human respiratory epithelial cells. *J. Immunol.* 186: 3484–3496.
35. Engeroff, P., F. Caviezel, D. Mueller, F. Thoms, M. F. Bachmann, and M. Vogel. 2020. CD23 provides a noninflammatory pathway for IgE-allergen complexes. *J. Allergy Clin. Immunol.* 145: 301–311.e4.
36. Zhao, J., L. Jiang, L. Deng, W. Xu, Y. Cao, C. Chen, Y. Yang, H. Wu, Y. Huang, Z. Zhu, and H. Huang. 2019. Important roles of CD32 in promoting suppression of IL-4 induced immune responses by a novel anti-IL-4Rα therapeutic antibody. *MAbs* 11: 837–847.
37. Punnonen, J., H. Yssel, and J. E. de Vries. 1997. The relative contribution of IL-4 and IL-13 to human IgE synthesis induced by activated $CD4^+$ or $CD8^+$ T cells. *J. Allergy Clin. Immunol.* 100: 792–801.
38. Kim, S. H., J. Y. Kim, H. J. Lee, M. Gi, B. G. Kim, and J. Y. Choi. 2014. Autoimmunity as a candidate for the etiopathogenesis of Meniere's disease: detection of autoimmune reactions and diagnostic biomarker candidate. *PLoS One* 9: e111039.
39. Hammad, H., and B. N. Lambrecht. 2015. Barrier epithelial cells and the control of type 2 immunity. *Immunity* 43: 29–40.
40. Geha, R. S., H. H. Jabara, and S. R. Brodeur. 2003. The regulation of immunoglobulin E class-switch recombination. *Nat. Rev. Immunol.* 3: 721–732.
41. Munno, I., V. Centonze, M. Marinaro, A. Bassi, G. Lacedra, V. Causarano, P. Nardelli, M. A. Cassiano, and O. Albano. 1998. Cytokines and migraine: increase of IL-5 and IL-4 plasma levels. *Headache* 38: 465–467.
42. Flook, M., L. Frejo, A. Gallego-Martinez, E. Martin-Sanz, M. Rossi-Izquierdo, J. C. Amor-Dorado, A. Soto-Varela, S. Santos-Perez, A. Batuecas-Caletrio, J. M. Espinosa-Sanchez, et al. 2019. Differential proinflammatory signature in vestibular migraine and Meniere disease. *Front. Immunol.* 10: 1229.
43. Møller, M. N., S. Kirkeby, and P. Cayé-Thomasen. 2017. Innate immune defense in the inner ear—mucines are expressed by the human endolymphatic sac. *J. Anat.* 230: 297–302.
44. Kaiserlian, D., A. Lachaux, I. Grosjean, P. Graber, and J. Y. Bonnefoy. 1993. Intestinal epithelial cells express the CD23/Fc epsilon RII molecule: enhanced expression in enteropathies. *Immunology* 80: 90–95.
45. Yang, P. C., M. C. Berin, L. C. Yu, D. H. Conrad, and M. H. Perdue. 2000. Enhanced intestinal transepithelial antigen transport in allergic rats is mediated by IgE and CD23 (FcεRII). *J. Clin. Invest.* 106: 879–886.
46. Hakonarson, H., C. Carter, C. Kim, and M. M. Grunstein. 1999. Altered expression and action of the low-affinity IgE receptor FεRII (CD23) in asthmatic airway smooth muscle. *J. Allergy Clin. Immunol.* 104: 575–584.
47. Aberle, N., A. Gagro, S. Rabatić, Z. Reiner-Banovac, and D. Dekaris. 1997. Expression of CD23 antigen and its ligands in children with intrinsic and extrinsic asthma. *Allergy* 52: 1238–1242.
48. Tantisira, K. G., E. S. Silverman, T. J. Mariani, J. Xu, B. G. Richter, B. J. Klanderman, A. A. Litonjua, R. Lazarus, L. J. Rosenwasser, A. L. Fuhlbrigge, and S. T. Weiss. 2007. FCER2: a pharmacogenetic basis for severe exacerbations in children with asthma. *J. Allergy Clin. Immunol.* 120: 1285–1291.
49. Yu, L. C. H., G. Montagnac, P. C. Yang, D. H. Conrad, A. Benmerah, and M. H. Perdue. 2003. Intestinal epithelial CD23 mediates enhanced antigen transport in allergy: evidence for novel splice forms. *Am. J. Physiol. Gastrointest. Liver Physiol.* 285: G223–G234.
50. Yokota, A., H. Kikutani, T. Tanaka, R. Sato, E. L. Barsumian, M. Suemura, and T. Kishimoto. 1988. Two species of human Fc epsilon receptor II (Fc epsilon RII/CD23): tissue-specific and IL-4-specific regulation of gene expression. *Cell* 55: 611–618.
51. Yu, P., M. Kosco-Vilbois, M. Richards, G. Köhler, and M. C. Lamers. 1994. Negative feedback regulation of IgE synthesis by murine CD23. *Nature* 369: 753–756.
52. Pforte, A., G. Breyer, J. C. Prinz, P. Gais, G. Burger, K. Häussinger, E. P. Rieber, E. Held, and H. W. Ziegler-Heitbrock. 1990. Expression of the Fc-receptor for IgE (Fc epsilon RII, CD23) on alveolar macrophages in extrinsic allergic alveolitis. *J. Exp. Med.* 171: 1163–1169.
53. Kilmon, M. A., R. Ghirlando, M. P. Strub, R. L. Beavil, H. J. Gould, and D. H. Conrad. 2001. Regulation of IgE production requires oligomerization of CD23. *J. Immunol.* 167: 3139–3145.
54. Defrance, T., J. P. Aubry, F. Rousset, B. Vanbervliet, J. Y. Bonnefoy, N. Arai, Y. Takebe, T. Yokota, F. Lee, K. Arai, et al. 1987. Human recombinant interleukin 4 induces Fc epsilon receptors (CD23) on normal human B lymphocytes. *J. Exp. Med.* 165: 1459–1467.
55. Li, H., M. Chehade, W. Liu, H. Xiong, L. Mayer, and M. C. Berin. 2007. Allergen-IgE complexes trigger CD23-dependent CCL20 release from human intestinal epithelial cells. *Gastroenterology* 133: 1905–1915.